LONG-PULSE ELM-FREE H-MODE REGIME WITH FEEDBACK-CONTROLLED DETACHMENT UNDER BORONIZED METAL WALL IN EAST

G.S. XU

Institute of Plasma Physics, Chinese Academy of Sciences

Hefei, China

Email: gsxu@ipp.ac.cn

G.F. Ding¹, G.J. Zhang^{1,2}, Y.F. Wang¹, X. Jian¹, T. Zhang¹, Z.Q. Zhou^{1,2}, K. Wu¹, Q.Q. Yang¹, R. Chen¹, L. Yu^{1,2}, L.Y. Meng¹, L. Wang¹, H.Q. Wang³, N.M. Li⁴, Z.Y. Lu¹, K.D. Li¹, S.Y. Ding³, X.Q. Xu⁴, N. Yan¹, L.Q. Xu¹, X. Lin¹, B. Zhang¹, J.P. Qian¹, T.F. Zhou¹, P. Li¹, C. Zhou², S.F Wang², Q. Zang¹, H.Q. Liu¹, F. Ding¹, L. Zhang¹, Y.F. Jin¹, Y.M. Duan¹, Y.W. Yu¹, R. Ding¹, G.Q. Li¹, X.Z. Gong¹, K. Lu¹, J.S. Hu¹, Y.T. Song¹, B.N. Wan¹

1 Institute of Plasma Physics, Hefei Institutes of Physical Science, Chinese Academy of Sciences, Hefei 230031, China

- 2 University of Science and Technology of China, Hefei 230026, China
- 3 General Atomics, P. O. Box 85608, San Diego, CA 92186 5608, USA
- 4 Lawrence Livermore National Laboratory, Livermore, California 94550, USA

Abstract

The international thermonuclear experimental reactor (ITER) is now considering to use tungsten as the material for plasma-facing components (PFCs) and operate in the so-called high-confinement mode (H-mode). Heat pulse eruptions caused by the plasma instability named the edge localized mode (ELM) pose a critical threat to the PFCs, which can lead to severe material damage and generate metallic impurities that contaminate the core plasma, rendering stable H-mode operation difficult. Therefore, ITER and future fusion reactors are desired to operate in a plasma regime without ELM but with good energy confinement, simultaneously coupled with the plasma detachment to relieve heat load on the material surface. However, such an operational regime has not yet been demonstrated for long pulse without expense of energy confinement, and the mechanism for maintaining ELM suppression in a detached H-mode plasma remains unclear. Here, we report the first demonstration of the achievement of a long-pulse detached H-mode plasma regime without ELM but with energy confinement even better than the standard H-mode in a metal-wall environment, and elucidate, for the first time, the underlying physics of such a long-pulse plasma regime. We find that a high-frequency broadband turbulence (HFBT) is excited in the plasma edge region that provides a radial transport channel, thus preventing ELM generation. HFBT is stabilized by collisionality and destabilized by electron temperature gradient, showing a nature of η_e -TEM. Additionally, HFBT can be destabilized by negative impurity density gradient. These characteristics of HFBT are suitable for ITER and future reactors. These findings may lead to a promising operational scenario for future tokamak fusion reactors compatible with metal-wall conditions, which is essential for harvesting fusion energy.

1. INTRODUCTION

Tungsten is the leading candidate for plasma-facing wall materials in future fusion reactors, mainly because of the restriction of the retention of the fusion fuel, i.e., tritium, in the material. ITER is now considering switching its plasma-facing wall material from beryllium to tungsten, using boron to coat the wall, and using electron cyclotron resonance heating (ECRH) to control tungsten impurity concentration in the plasma [1]. However, the tungsten impurity can become a severe radiator of plasma energy, dilute the fuel ions, and degrade the plasma energy confinement. Further, even very low concentrations of tungsten impurities of ~10 ppm in the plasma core can have a significant impact on plasma confinement, making it much more difficult to maintain a stable, high-performance plasma. Whether switching to tungsten walls will make it difficult for ITER to achieve its scientific goals has presently become the biggest concern [1]. Thus, a plasma operational regime suitable for tungsten wall and long-pulse operation is urgently needed for ITER and future fusion reactors, which is able to reduce the heat flow to the wall and enhance the outward transport of impurities so that low tungsten concentrations and high energy confinement can be achieved simultaneously. Recently, the EAST superconducting tokamak has achieved, for the first time, a long-pulse plasma operational regime that meets the above requirements under the metal wall with boronization conditions, as to be adopted by ITER, on a time scale of ≥50 s.

The divertor is the region in which the plasma is in direct contact with the material surface. It is widely recognized that the divertor of future fusion reactors will necessarily operate in a detachment state to dissipate a significant fraction of the energy inside the divertor, i.e., by injecting low-Z impurities into the plasma, and this, along with neutral particles recycling from the surface, reduces the heat and particle flows reaching the surface of the divertor target plates. Otherwise, sputtered tungsten and resulted damages would be intolerable in future fusion reactors. However, the operation of divertor detachment is required to be compatible with the so-called high-confinement mode (H-mode) to minimize the size and cost of the device, which poses a serious and long-standing challenge. H-mode features a transport barrier, called the pedestal, which is spontaneously formed at the plasma edge with steep plasma density and temperature gradients, resulting in a significant improvement in the plasma energy confinement with respect to the low confinement mode (L-mode). The pedestal is prone to a plasma instability called the edge localized mode (ELM), leading to the periodic collapse of the pedestal, generating large transient heat and particle flows, which erode the walls facing the plasma - a major source of metallic impurities. Therefore, ITER and future fusion reactors are desired to operate in an H-mode regime where ELMs are fully suppressed, yet with better energy confinement performance than that of the standard H-mode, i.e., $H_{98v2} > 1$, where H_{98v2}, named the H-factor, is the plasma energy confinement enhancement factor relative to the international tokamak energy confinement scaling. The experimental demonstration of this operational regime in long pulses is of great significance in enhancing confidence in ITER's ability to achieve its scientific goals under full-metal-wall conditions.

Recently, ELM-suppressed H-mode plasmas with divertor detachment have been achieved in AUG [2,3], DIII-D [4,5] and JET [6] tokamaks. However, the ELM suppression is only obtained for short period and associated with a reduction in pedestal pressure and density, and a degradation in energy confinement. It remains yet to be experimentally verified whether the simultaneous realization of ELM-free regime and divertor detachment with good energy confinement can be maintained on long time scales in a metal wall environment. Since a large amount of impurities was injected in these experiments to achieve divertor detachment, it is a great challenge to exhaust the impurities in order to achieve steady state operation in long pulses. This would require a new transport channel across the pedestal that is capable of continuously exhausting impurities and avoiding further growth of the pedestal beyond the stability boundary to maintain a steady state.

In the new experiments in EAST reported here, a long-pulse stable ELM-free H-mode regime has been obtained with the nitrogen seeding, which is observed to lead to the improvement of the global energy confinement, increase in the pedestal pressure and excitation of a high-frequency turbulence in the pedestal steep gradient region, identified as the temperature-gradient-driven trapped electron modes (η_e -TEM) [7]. The TEM provides a radial transport channel for particles, as suggested by high-fidelity gyrokinetic simulations. This newly identified key underlying physics mechanism will facilitates the long-pulse operations of future fusion reactors with metal walls.

2. EXPRIMENTAL RESULTS

2.1. SHORT-PULSE ELM-FREE H-MODE WITH DIVERTOR DETACHMENT VIA FEEDBACK-CONTROLLED N_2 SEEDING.

2.1.1. Time traces

EAST is a superconducting tokamak with full-metal walls, and all plasma-facing components (PFCs) are actively water-cooled. Boronization wall coating has now being applied to provide timely information for the consideration of switching the first wall of ITER to tungsten. Under boronized full-metal wall and ECRH dominated electron heating conditions similar to ITER, EAST has achieved a high-performance ELM-free H-mode plasma with divertor detachment. We first obtained this plasma regime in a short-pulse discharge as shown in Fig. 1 at $q_{95} = 5.2$, which is the same as in the ITER steady-state scenario, where q_{95} is the safety factor at the 95% of total flux surface. The detailed parameters of this discharge are shown in Methods. The outer striking point of the lower divertor was located at the horizontal target plate. Nitrogen (N₂) gas was injected from the outer horizontal target plate of the lower divertor. The electron temperature, T_{et} , measured by divertor target Langmuir probes, was first used to determine the onset of detachment, and then switched to the feedback control of one channel of absolute extreme ultraviolet (AXUV) radiation signal near the lower X point via seeding pulse width modulation (Fig. 1b) to maintain detachment. The divertor detachment was achieved as T_{et} at the outer target plate of the lower divertor was maintained below 5 eV.

Note that this experiment was carried out on the 4th day after the boronization with the evaporation of 10g C2B10H12 carbaborane solid. Following three days of high-power discharges, the boron film on the walls produced by boronization was nearly eroded away, resulting in essentially uncoated metal walls, similar to the situation for ITER, as the boron film will be eroded away much more quickly in ITER, leaving essentially uncoated metal walls [1].

Prior to N_2 seeding, large ELMs appeared intermittently, as indicated by divertor $D\alpha$ signal (Fig. 1d), with relatively poor plasma energy confinement at H_{98y2} =0.8-0.9. During N_2 seeing, firstly, the duration of ELM-free period between two clusters of ELMs was prolonged, and finally, the plasma became completely ELM-free; the plasma energy confinement was

significantly improved with H_{98y2} gradually increasing and finally reaching 1.2 (Fig. 1e). Meanwhile, the plasma stored energy (Fig. 1a), as well as the electron and ion temperatures on axis increased significantly (Fig. 1g). After the complete disappearance of ELMs, the central-line-averaged electron density, n_{el} , and line-averaged electron density across the pedestal top, n_{eledge} , began to decrease (Fig. 1a). Note that there is no density feedback control in this discharge. The impurity radiations of tungsten, molybdenum, copper and iron in the plasma core region, as well as the total radiation power, were significantly reduced (Fig. 1f), suggesting that this plasma regime exhibits an excellent particle exhaust capability.

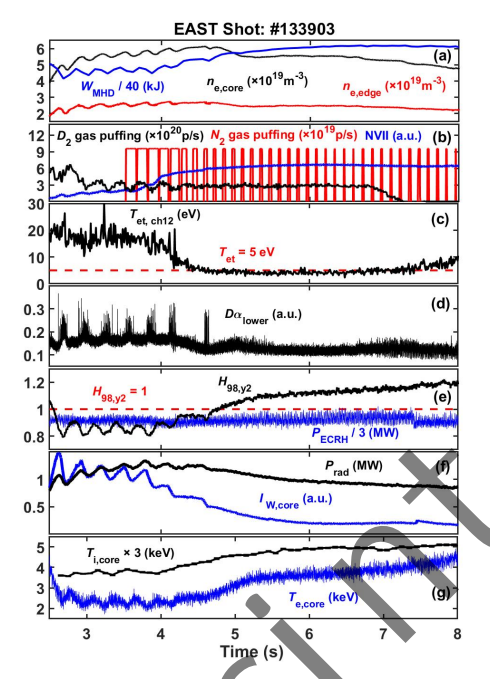


Fig. 1 An ELM-free H-mode plasma, #133903, at q_{95} =5.2 with divertor detachment being achieved by nitrogen seeding and X-point AXUV radiation feedback control in EAST with boronized metal wall. (a) Plasma stored energy (blue), central-line-averaged electron density across the pedestal top (red) measured by a polarization interferometer; (b) Nitrogen injection rate from the lower divertor with pulse width modulation (red), total deuterium injection rate (black) and nitrogen NVIL line emission from the plasma core measured by an extreme ultraviolet (EUV) spectrometer (blue); (c) Electron temperature measured by divertor Langmuir probe channel 12 at bottom of the vertical target plate; (d) D α line emission from lower divertor; (e) Energy confinement enhancement factor H_{98y2} (black) and ECRH injected power (blue); (f) Total radiation power from the plasma confinement region measured by bolometer arrays (black) and tungsten line emission from the plasma core measured by an EUV spectrometer (blue); (g) Electron temperature on axis (blue) measured by an ECE diagnostic and ion temperature on axis (black) measured by a X-ray crystal spectrometer.

2.1.2. Profile changes and stability analysis

Comparative profile analysis before and during N_2 seeding (at 3.42 s and 6.15s, respectively) revealed key changes. The pedestal n_e gradient decreased slightly, while the pedestal T_e gradient increased significantly (Fig. 2a). The electron temperature in the pedestal top region increase nearly double, which may be responsible for the enhanced energy confinement, as shown in Fig. 2b. The peak $E \times B$ velocity in the pedestal, measured via Doppler backscattering (DBS) increased from 1.4 km/s to 3.5 km/s (in the electron diamagnetic direction), as shown in Fig. 2c. In the divertor, the peak ion saturation current density J_{sat} near the strike point (2.6 cm from the corner along the horizontal target plate), exhibiting a substantial reduction with N_2 seeding (Fig. 2d). The peak T_{et} location is observed on the vertical target plate (Fig. 2e), which may be attributed the enhanced radiative cooling near the horizontal target plate of the EAST lower tungsten divertor, where neutral particles accumulate through target-plate reflection. The peak T_{et} near the strike point decreased from 15 eV to below 5 eV, and the peak T_{et} also dropped to \sim 5 eV. The peak vertical heat flux q_t profile flattened and the peak q_t dropped about 90% (Fig. 2f), indicating effective mitigation of the high heat load on the divertor target.

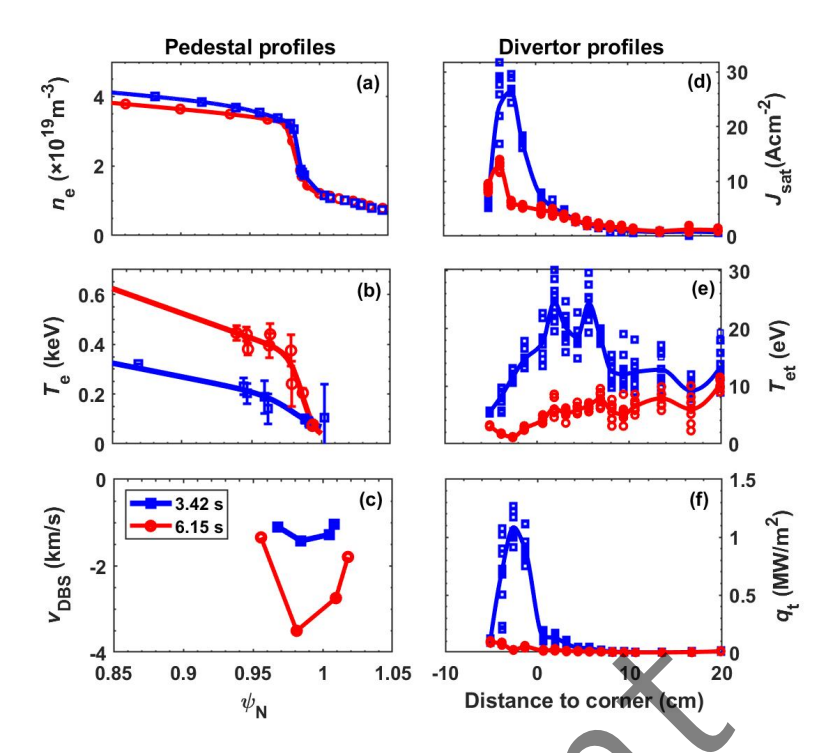


Fig. 2 Pedestal (left) and divertor (right) profiles for attached (blue) and detached (red) divertor. (a) Electron density profiles measured by sweep-frequency reflectometer; (b) Electron temperature profiles measured by Thomson Scattering (TS); (c) Perpendicular propagation velocity measured by DBS; (d)-(f) Divertor particle flux, electron temperature and vertical heat flux measured by divertor Langmuir probe.

Figure 3(a) shows the results of the linear stability analysis of the pedestal ideal peeling-ballooning (PB) modes using ELITE code. Prior to N_2 seeding, the pedestal is in the PB mode deeply stable region. However, the intermittent bursts of ELM clusters were observed during the experiment, which may be associated with resistive non-ideal magnetohydrodynamics (MHD) effects, such as resistive ballooning modes. As calculated by BOUT++ code, shown in Fig 3(b), the instabilities appear and the linear growth rates peak at n \sim 20 as the effects of resistivity are taken into account. During N_2 seeding, ELITE shows that pedestal is close to the corner between the peeling boundary and the ballooning boundary. To maintain the pedestal near the instability boundary for long pulse operation, it requires a transport channel across the pedestal to avoid further growth of the pedestal beyond the instability boundary; such a transport channel may be provided by pedestal turbulence as shown below.

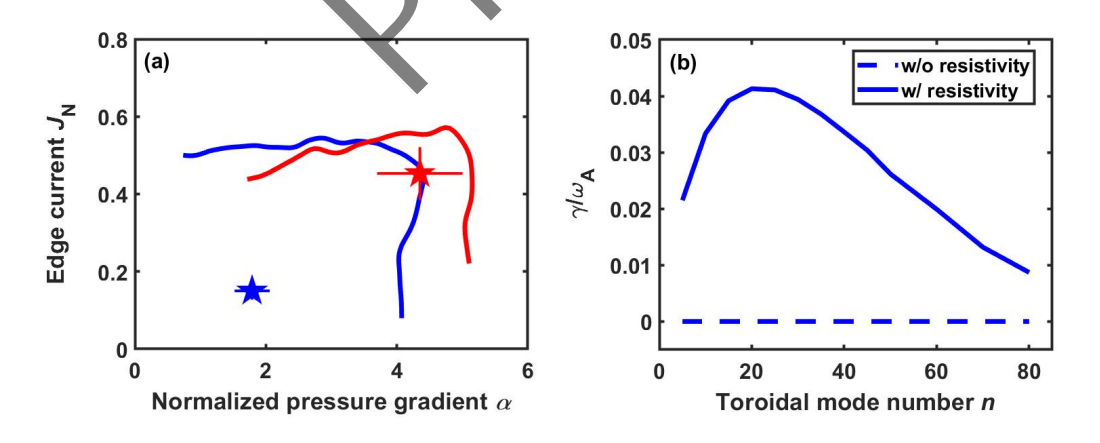


Fig. 3 (a) Linear stability analysis of the pedestal ideal PB modes before N_2 seeding (blue) and after N_2 seeding (red) using the ELITE code. (b) The blue dashed and blue solid lines represent the linear growth rates calculated using the BOUT++ code, with the former using the ideal PB model and latter taking into account the effects of resistivity.

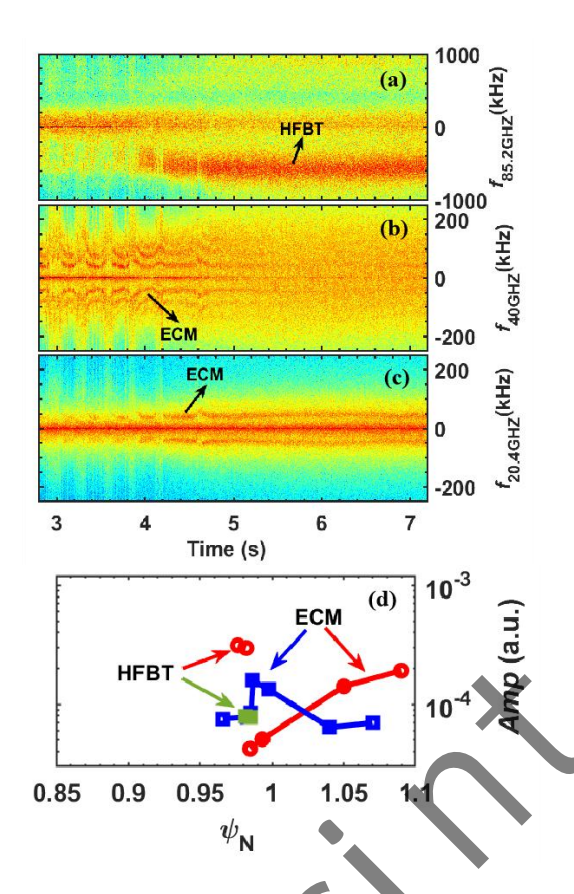


Fig. 4 Frequency spectra measured by a multichannel poloidal correlation reflectometer at (h) 85.2 GHz; (i) 40 GHz; (j) 20.4 GHz, respectively; (d) The amplitude of ECM and HFBT calculated from the multichannel poloidal correlation reflectometer.

Before N_2 seeding, a newly high frequency broadband turbulence (HFBT) appears with a frequency of about 200-500kHz. During N_2 seeding, HFBT intensified and its frequency upshift to 400-700 kHz, propagating in the electron diamagnetic direction, appears in the upper portion of the pedestal region, as shown in Fig. 4(a). It was not visible to the high-frequency Mirnov magnetic coils, suggesting that it could be an electrostatic mode. In the lower region of the pedestal and in the SOL, a mode at a frequency of ~40 kHz with multiple harmonics is present in the ELM-free phases, which is ECM, usually seen in the H-mode pedestal region of EAST at high collisionality, which was identified as DTEM [8]. The amplitude profiles of ECM and HFBT are measured by the multichannel poloidal correlation reflectometer with the calculation: $Amp = \sum_{f_{lower}}^{f_{upper}} S_a(f) - S_a^{backgroud}(f)$, where f_{lower} to f_{upper} represent the frequency bandwidth of the the mode, $S_a(f)$ represents the auto-power spectra during the mode excitation period, and $S_a^{backgroud}(f)$ represents the background level of the channel. The peak amplitude of ECM moves from the pedestal steep gradient region to the SOL region, whereas the HFBT maintained its position in the upper portion of the pedestal region throughout the N_2 seeding phases (Fig. 4d).

2.2. LONG-PULSE ELM-FREE H-MODE PLASMA WITH FEEDBACK-CONTROLLED DIVERTOR DETACHMENT VIA NITROGEN SEEDING IN THE EAST TOKAMAK UNDER THE BORONIZED METAL WALL ENVIRONMENT

With plasma current, I_p , reduced from 500 kA to 400/350 kA ($q_{95} = 6.2/6.8$), long-pulse discharges of 50 - 70 s (limited by volt-seconds) have been achieved in this new stationary ELM-free H-mode regime with divertor detachment and enhanced confinement at $H_{98y2} \sim 1.1$. Fig 5 shows such a typical discharge of 50 s at $q_{95} = 6.2$. By feedback control with the supersonic molecular beam injection (SMBI) from the outer midplane, n_{el} was maintained stably at 4×1019 m-3, which is \sim 61% of the Greenwald density [35] (Fig. 5a). Stable detachment at both the inner and outer target plates of the lower divertor was achieved by feedback control of T_{et} on the outer divertor target plate [36]. T_{et} at the horizontal target plate of the lower divertor was reduced to \sim 2 eV (Fig. 5c) and the divertor peak surface temperature measured by an infrared camera was reduced from \sim 500°C to \sim 250°C. The loop voltage did not rise significantly after N_2 seeding and remained at \sim 0.08 V.

The tungsten impurity source from the divertor was significantly suppressed, as indicated by the tungsten WI line emission from the lower divertor. However, the tungsten and molybdenum line emissions from the plasma core region continue to increase until \sim 40 s before reaching saturation, while the carbon line emission keeps nearly constant, the total radiation power Prad does not increase significantly and the effective charge number $Z_{\rm eff}$ is maintained near 2.2. The

increased metallic impurities are mainly due to the enhanced sputtering of the limiters by nitrogen impurity ions, rather than from the divertors.

As can be seen in Fig. 5(d), before N_2 seeding, grassy-ELM-like perturbations appear in the divertor $D\alpha$ signals. Then, the perturbations are completely suppressed and an ELM-free regime is maintained till the end of the discharge. The divertor $D\alpha$ drops sharply when N_2 injection begins and then continues to decrease. At the same time, the total D_2 injection rate also continues to decrease (Fig. 5d). The pedestal top n_e exhibits little changes due to feedback control, but n_e in the SOL significantly decreases. These observations suggest a reduction in the particle recycling from the walls and an increase in the density gradient at the pedestal.

HFBT was also observed in the pedestal region with a frequency of about 350 kHz before N_2 seeding, and then the HFBT frequency shifted upwards to 550 kHz during N_2 seeding. During N_2 seeding, the high-frequency turbulence with a peak frequency at ~550 kHz also appears (Fig. 5f), at the pedestal region. However, different from the discharge #133903, the ECM was not detected in either the pedestal or SOL regions throughout the whole discharge, indicating that the HFBT plays important role for exhausting both continuously seeded nitrogen impurities and sputtered metallic impurities during this long-pulse ELM-free operation.

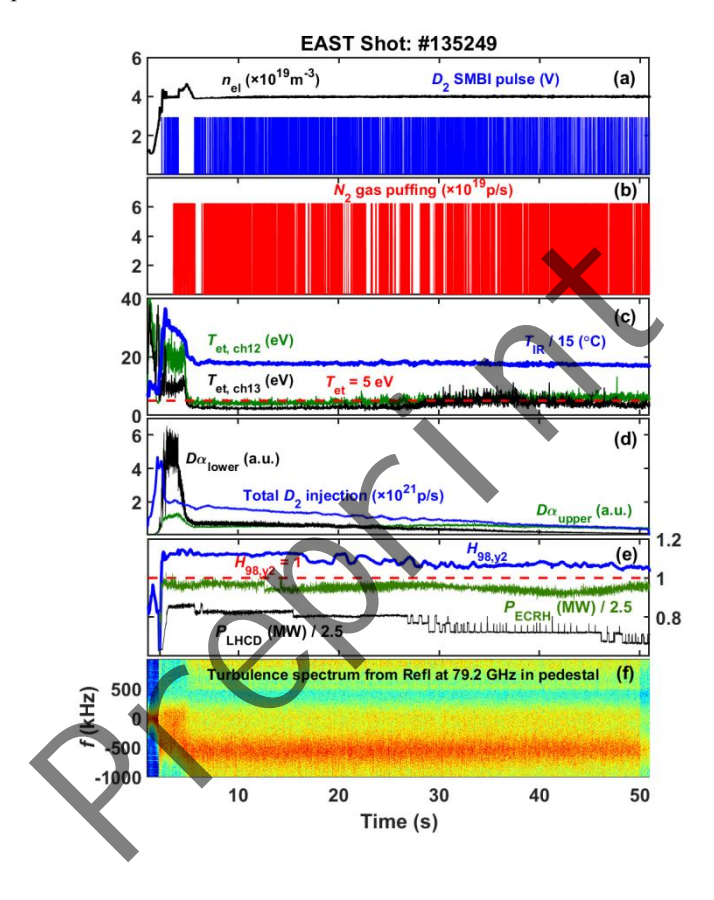


Fig. 5 A long-pulse ELM-free H-mode plasma of \sim 50s, #135249, with feedback-controlled divertor detachment via nitrogen seeding in the EAST tokamak under the boronized metal wall environment. (a) Central-line-averaged electron density (black) and deuterium SMBI pulses for density feedback control (blue); (b) Nitrogen injection rate from the lower divertor with pulse width modulation; (c) Electron temperature measured by divertor Langmuir probe channel 12 at the bottom of the vertical target plate (green) and channel 13 at the horizontal target plate (black) near the right-angle corner of the lower outer divertor, divertor peak surface temperature measured by an infrared camara (blue); (d) D α line emission from lower divertor (black) and upper divertor (green) and total deuterium gas injection rate (blue); (e) Energy confinement enhancement factor H_{98y2} (blue) and Injected power of ECRH (green) and lower hybrid current drive (LHCD) (black); (f) Frequency spectrum measured by a channel of the multichannel poloidal correlation reflectometer at 79.2 GHz.

2.3. SIMULATION OF EAST PEDESTAL TURBULENCE USING CGYRO CODE

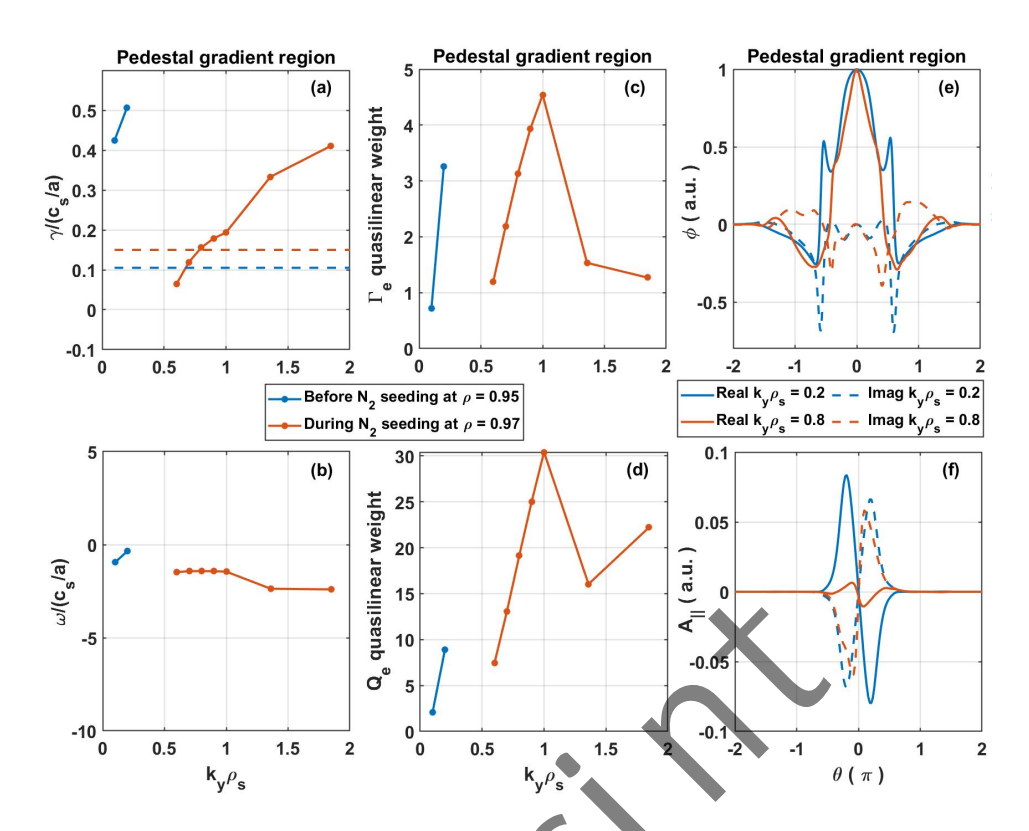


Fig. 6 Gyrokinetic analysis of the pedestal of shot #133903 in EAST, as carried out using CGYRO code. The plasma parameters before and during N_2 seeding are indicated by blue and red curves, respectively. The radial positions calculated before N_2 seeding are $\rho=0.95$ in the pedestal gradient region and $\rho=0.88$ at the pedestal top. The radial positions calculated during N_2 seeding are $\rho=0.97$ in the pedestal gradient region and $\rho=0.94$ at the pedestal top. (a) Real frequency and (b) linear growth rate normalized by c_s/a as a function of $k_y\rho_s$ with dashed lines indicating local E×B shearing rates, as well as the quasilinear weights of (c) electron particle flux and (d) electron heat flux in the pedestal gradient region. The real and imaginary parts of (e) electrostatic potential and (f) parallel magnetic vector potential eigenfunctions as a function of the extended ballooning angle θ at $k_y\rho_s=0.2$ before N_2 seeding and $k_y\rho_s=0.8$ during N_2 seeding.

In order to understand the nature of the newly observed high-frequency turbulence mode in the long-pulse ELM-free regime in EAST, linear gyrokinetic simulation of the pedestal is performed using a high-fidelity code CGYRO. The experimentally measured profiles shown in Fig. 6 for shot #133903 and the magnetic equilibrium calculated by high-resolution kinetic EFITs are used as inputs to the CGYRO simulations (See Methods for detailed analysis). The simulation results indicate the presence of η_e -TEM in the pedestal gradient region in the intermediate $k_y \rho_s = 0.6$ -3.4 range during N_2 seeding, with the linear growth rate exceeding the local E×B shear rate, which is destabilized by temperature gradients, in good agreement with the most features of the experimentally observed high-frequency turbulence. Furthermore, CGYRO simulations show that this mode drives radially outward particle and electron heat fluxes, providing a radial transport channel across the pedestal, which may be responsible for the ELM suppression. In addition, before N_2 seeding in the pedestal gradient region, the simulations show a low-frequency mode in the low $k_y \rho_s = 0.1$ -0.2 range, consistent with the turbulence scale of the ECM seen in the experiments [8].

3. SUMMARY AND CONCLUSIONS

Elimination of large ELMs is the key to achieving stable high-performance operation in long pulses under full-metal-wall conditions. H-mode under the condition of divertor detachment with impurity seeding is expected to be the routine operational scenario for ITER. If spontaneous ELM suppression can be achieved at the same time, this stationary H-mode regime would be a desirable option. The key to its access usually requires a turbulent or quasi-coherent mode in the steep gradient region of the pedestal, providing a particle and heat transport channel to limit the growth of the gradient and height of the pedestal beyond the PB-mode stability boundaries, thus avoiding ELMs. Under metal-wall conditions, it is particularly important to provide an exhaust channel for

IAEA-CN-316/ EX/P7-23

impurities across the pedestal to avoid accumulation of metallic impurities in the plasma core, which can degrade the energy confinement.

The newly demonstrated long pulse high-performance regime in EAST, where pedestal turbulence replaces ELMs in H-mode plasmas with feedback-controlled divertor detachment, provide a promising solution for ITER and future fusion reactors to achieve long-pulse stable operations under full-metal-wall conditions. HFBT, which may be suitable for ITER pedestal region due to its η_e -TEM nature, may render large ELMs to disappear naturally, and thus the current widespread concerns about ELM control reliability and core metal impurity accumulation may not pose a major obstacle for ITER to achieve its fusion gain Q = 10 goal.

ACKNOWLEDGEMENTS

This work was supported by the National Magnetic Confinement Fusion Energy Program of China under Grant No. 2019YFE03030000 and the National Natural Science Foundation of China under Grant No. U19A20113.

REFERENCES

- [1] A. Loarte, et al. Initial evaluations in support of the new ITER baseline and Research Plan. ITER technical report No. ITR-24-004.
 - https://www.iter.org/doc/www/content/com/Lists/ITER%20Technical%20Reports/Attachments/25/ITR-24-004-Baseline-ok.pdf
- [2] A. Kallenbach, et al. Developments towards an ELM-free pedestal radiative cooling scenario using noble gas seeding in ASDEX Upgrade. Nucl. Fusion **61**, 016002 (2021).
- [3] M. Bernert, et al. X-point radiation, its control and an ELM suppressed radiating regime at the ASDEX Upgrade tokamak. Nucl. Fusion 61, 024001 (2021).
- [4] L. Wang, et al. Integration of full divertor detachment with improved core confinement for tokamak fusion plasmas. Nat. Commun. 12, 1365 (2021).
- [5] D. G. Wu, et al. Compatibility of divertor detachment and ELM suppression in DIII-D high-p plasmas with ITER-similar shape. Nucl. Fusion 64, 086042 (2024).
- [6] S. Glöggler, et al. Characterisation of highly radiating neon seeded plasmas in JET-ILW. Nucl. Fusion 59, 126031 (2019).
- [7] J. Y. Kim and H. S. Han, Linear interaction and relative role of the ion temperature gradient and trapped electron modes in the reactor-relevant finite beta plasma condition. Phys. Plasmas 24, 072501 (2017).
- [8] H. Q. Wang, et al. New Edge Coherent Mode Providing Continuous Transport in Long-Pulse H-mode Plasmas. Phys. Rev. Lett. 112, 185004 (2014).